ELSEVIER

Journal of Chromatography A, 953 (2002) 55–66

JOURNAL OF CHROMATOGRAPHY A

www.elsevier.com/locate/chroma

Study of the adsorption equilibria of the enantiomers of 1-phenyl-1-propanol on cellulose tribenzoate using a microbore column

Alberto Cavazzini[a,b], Attila Felinger[a,b,1], Krzystof Kaczmarski[a,b,2], Pawel Szabelski[a,b], Georges Guiochon[a,b,*]

[a]*Department of Chemistry, University of Tennessee, 552 Buehler Hall, Knoxville, TN 37996-1600, USA*
[b]*Division of Chemical and Analytical Sciences, Oak Ridge National Laboratory, Oak Ridge, TN, USA*

Received 3 September 2001; received in revised form 28 January 2002; accepted 7 February 2002

Abstract

Using competitive frontal analysis, the binary adsorption isotherms of the enantiomers of 1-phenyl-1-propanol were measured on a microbore column packed with a chiral stationary phase based on cellulose tribenzoate. These measurements were carried out using only the racemic mixture. The experimental data were fitted to four different isotherm models: Langmuir, BiLangmuir, Langmuir–Freundlich and Tóth. The BiLangmuir and the Langmuir–Freundlich models accounted best for the competitive adsorption data. An excellent agreement between the experimental and the calculated overloaded band profiles for various samples of racemic mixture was obtained when the equilibrium dispersive model of chromatography was used together with the BiLangmuir competitive isotherm. The isotherm parameters measured under competitive conditions were used to calculate the overloaded band profiles of large samples of the pure *S*- and *R*-enantiomers, too. A satisfactory agreement between the experimental and calculated band profiles was observed when using in the computation the corresponding single component BiLangmuir isotherm derived from the binary isotherm previously determined. Thus only data derived from the racemic mixture are required for computer optimization of the preparative chromatography separation of the enantiomers.

Keywords: Enantiomer separation; Adsorption equilibria; Chiral stationary phases, LC; Adsorption isotherms; 1-Phenyl-1-propanol; Cellulose tribenzoate

1. Introduction

Large-scale preparative HPLC has become the preferred method for the separation and purification of enantiomers [1]. This method is expensive, however, and the separation factors are usually small or moderate. Therefore, computer-assisted optimization of the experimental conditions under which to operate the separation process could save significant amounts of time and money. This requires the prior determination of the physico-chemical properties of the phase system selected. This study is usually carried out on a scaled-down system. The adsorption isotherm data measured at this lower scale are used

*Corresponding author. Tel.: +1-865-9740-733; fax: +1-865-9742-667.

E-mail address: guiochon@utk.edu (G. Guiochon).

[1]Present address: Department of Analytical Chemistry, University of Veszprem, P.O. Box 158, H-8201 Veszprem, Hungary.

[2]Present address: Faculty of Chemistry, Rzeszow University of Technology, W. Pola 2 Street, 35-959 Rzeszow, Poland.

0021-9673/02/$ – see front matter
PII: S0021-9673(02)00150-4

to calculate the separation under overloaded conditions [2]. The classical approach for the determination of competitive isotherm consists in making systematic measurements of isotherm data with the pure components and several mixtures of different relative concentrations [2]. Enantiomers at a high purity degree are generally extremely expensive or just not available. Therefore, we need methods that could be used with the single racemic mixture, usually much cheaper and more readily available, and would need only small amounts of sample. The use of capillary columns instead of standard analytical columns in gas chromatography was shown to be a useful alternative for measuring the adsorption data needed for the optimization of the preparative scale separations [3,4]. An important reduction of the measurement cost arose from large decreases of the amounts of sample and of stationary phase needed.

Unfortunately, several serious technical problems have long made this approach difficult if not practically impossible to implement in HPLC. Flow rate stability and reproducibility is poor at flow-rates smaller than 5–10 μl/min. Extra-column holdup volumes often dramatically affect the performance of separations carried out in miniaturized systems [5,6]. The recent development of commercial HPLC instruments dedicated to the use of capillary or microbore columns, however, has markedly improved the situation. Flow rate stability and reproducibility, even at very low flow-rates, is no longer a significant issue. The retention and band-broadening contributions of the extra-column holdup volumes are usually extremely reduced. The most serious remaining problems arise from the compromises that had to be made in the design of these modern instruments (see later). Recently, Jandera et al. [7] compared the adsorption isotherms of benzophenone, *o*-cresol, phenol and of the enantiomers of mandelic acid measured using microbore and conventional analytical HPLC columns, by the frontal analysis (FA) technique [2]. A good agreement was observed between the values of the parameters of the isotherm model measured under these different experimental conditions. The primary aim of this paper is the determination of the adsorption equilibrium data for the enantiomers of 1-phenyl-1-propanol (PP) on cellulose tribenzoate CSP, using a microbore HPLC column. We want also to confirm that, in many cases, isotherm data obtained with the racemic mixture can be used with mixtures of the enantiomers having any relative composition [8].

2. Theoretical

The chromatographic process can be described by several different mathematical models [2]. The equilibrium dispersive (ED) model is most often used when the mass transfer resistances are small. It is correct when mass transfer is controlled by diffusion in the mobile phase while the exchange of the eluates between mobile and stationary phase is fast. In this case, all the nonequilibrium contributions can be lumped into an apparent axial dispersion term. Because modern HPLC columns are characterized by high efficiency values, this model gives frequently excellent results, especially for the separation of relatively small molecules. In this case, the apparent dispersion coefficient is independent of the solute concentration in a sufficiently wide concentration range and nearly independent of its nature. Frequently, however, the kinetics of adsorption–desorption of the second enantiomer is too slow for the band profile of this compound to be accurately accounted for by the ED model [2]. For each component i in the column, the ED model includes the following mass balance equation:

$$\frac{\partial C_i}{\partial t} + F\frac{\partial q_i}{\partial t} + u\frac{\partial C_i}{\partial z} = D_{L,i}\frac{\partial^2 C_i}{\partial z^2} \quad (1)$$

where t and z are the time elapsed from the injection and the distance traveled by the molecules inside the column, respectively; u is the interstitial mobile phase velocity; C_i is the mobile phase concentration in equilibrium with the solid-phase concentration q_i, via an adsorption model isotherm ($q_i = f(C_1, C_2, \ldots, C_i, \ldots)$); F is the phase ratio, with $F = (1-\epsilon)/\epsilon$, ϵ being the total porosity, and $D_{L,i}$ is the apparent dispersion coefficient, defined according to:

$$D_{L,i} = \frac{H_i L}{2t_0} = \frac{H_i u}{2} \quad (2)$$

In Eq. (2), H_i represents the height equivalent to a theoretical plate (HETP) measured under linear conditions [2], L is the column length, and t_0 the

holdup time of the column ($t_0 = L/u$). In practice, it is assumed that all compounds have the same HETP.

Suitable initial and boundary conditions are necessary to solve Eq. (1). The following equations were used [9,10]:

Initial condition: $C_i(0, z) = 0$; (a)

Boundary condition at the column inlet

$(t > 0 \text{ and } z = 0)$: $C_i(t, 0) = C'_{f,i}$ (b-1)

where $C'_{f,i}$ is defined according to:

$$C'_{f,i} = \begin{cases} C_{f,i} & \text{if } 0 < t < t_p \\ 0 & \text{if } t_p < t \end{cases}$$

t_p being the injection time and the subscript f indicating an ''inlet value''. In the calculations made in this paper, the more rigorous Danckwerts condition (which accounts for the effect of axial diffusion during the very injection) was not used; in fact, it has been shown that when the column efficiency exceeds a few hundred plates (which is the case of the present study) the differences between the profiles calculated by using the Danckwerts condition or Eq. (b-1) are negligible [2].

Boundary condition at the column outlet

$$(t > 0 \text{ and } z = L): \frac{\partial C_i}{\partial z} = 0 \quad \text{(b-2)}$$

The ED model was solved using a program based on implementations of the method of orthogonal collocation on finite elements [2,11,12]. The set of discretized ordinal differential equations was solved with the Adams–Moulton method, implemented in the VODE procedure [13]. The relative and absolute errors of the numerical calculations were equal to 1×10^{-6} and 1×10^{-8}, respectively.

3. Experimental

3.1. Equipment

A 1100 Series Capillary Chromatograph (Agilent Technologies, Palo Alto, CA, USA) was used for all the experimental determinations. The instrument was equipped with a micro diode-array detector (cell volume, 500 nl), a flow splitter with an electromagnetic proportional valve connected to a flow sensor device (standard design of the Capillary 1100 Series) and a computer data station.

Our initial plan was to use the instrument in the same way as we did with the HP 1090 and HP 1100 to carry out FA measurements. One pump of the solvent delivery system pumps the pure mobile phase, the second one pumps a solution of the sample in the same mobile phase, at a suitable concentration. At a given period, the solvent delivery system generates a +10% step gradient of the second solution into the first. This provides for the input required for step FA. It became rapidly obvious, however, that the new instrument could not be used this way. The holdup volume between the entrance to the mixing chamber and the column is much too large (more than 300 μl) and step injected is too gradual to allow meaningful FA measurements. So, the instrumental arrangement had to be modified. Only one channel was used, connected to a six-way micro-valve (VICI, Cheminert CDX 0088, Valco Instrument, Houston, TX, USA) via 25-μm I.D. fused-silica capillaries (home made). An FA step is obtained by injecting a sufficiently large volume of a solution of the sample at suitable concentration into the stream of mobile phase. This was necessary in order to reduce the system dead volume and to create a back pressure (at least 10 bar) sufficiently large for the flow-rate controller to work properly. This new arrangement is the only one that we found possible under our experimental conditions. Its inconveniences are obvious. First, the main advantage of carrying out FA measurements of adsorption isotherm data using a two-pump system is lost. It is necessary to prepare sample solutions in advance, causing losses of precision, accuracy, time, and products. The former two are explained by minor flow-rate fluctuations associated with the injection of the large sample volumes required to carry out FA measurements. When the injection was performed, the back pressure into the system dropped by about 10% and the flow-rate fluctuated slightly. This observation may be ascribed in part to the compressibility of the liquid in the sample [14–16], although in this case (pressure $\simeq$ 20 bar), this phenomenon is expected to be too small to account for the whole effect noted. Steel sample loops of different volumes

(5, 10 and 250 μl) were used for the FA analysis and for the injection of the samples needed to generate band profiles. The micro-valve was operated by software (Ultra Plus II, Pump Controller Module-Interface Module; Micro-Tech Scientific, Sunnyvale, CA, USA). The system holdup volume measured under these conditions was 3±0.1 μl.

3.2. Materials

3.2.1. Mobile phase and chemicals

The mobile phase was a solution of *n*-hexane and 2-propanol (97:3, v/v). Hexane and 2-propanol were HPLC-grade solvents from Fisher Scientific (Fair Lawn, NJ, USA). All the solvents were filtered (0.2 μm Gelman Sciences, Ann Arbor, MI, USA) before use. 1,3,5-tri-*tert.*-butylbenzene (TTB) was purchased from Aldrich (Milwaukee, WI, USA). The racemic mixture of PP, also from Aldrich, was previously purified in our laboratory [17]. The single enantiomers (S-PP and R-PP) were obtained in a very small amount (a few mg) by collecting the corresponding fractions eluting from an analytical column [10].

3.2.2. Column

A 15×0.1-cm stainless steel column packed with Chiracel OB (cellulose tribenzoate coated on a silica support; Daicel, Tokyo, Japan) was used for all the measurements. The column was packed by Micro-Tech Scientific. The average size of the packing material particles was 20 μm. The total porosity, measured by injecting TTB, was 0.795. The column holdup time was 18.7 min. The efficiency of the column at a flow-rate of 5 μl/min of the mobile phase was about 1200 theoretical plates.

3.3. Procedure for isotherm determination

3.3.1. Measurements of experimental data

The competitive isotherm data were measured by FA, at 25.0±0.1°C and at a mobile phase flow-rate of 5 μl/min. The retention factors for the less, S-PP, and the more, R-PP, retained compound were, respectively, 1.66±0.01 and 2.10±0.01. The selectivity factor was $\alpha = 1.26$. The wavelength used for the FA measurements was 280 nm. The overloaded profiles were recorded at 254 and 270 nm. The volume necessary to reach the intermediate concentration plateau inside the column was 250 μl. After each new injection of a solution of sample in the mobile phase, the column was re-equilibrated with pure mobile phase (no staircase FA). The isotherms were measured up to a concentration of approximately 0–6 g/l total racemic mixture. Twenty data points were collected and all the measurements were repeated two times. Their average value was used for the determination of the isotherm parameters.

4. Results and discussion

The validation of any non-linear isotherm model requires a comparison of the overloaded band profiles recorded under well-defined experimental conditions and the profiles calculated with the isotherm model under the same conditions. It is well known, that different adsorption isotherms can fit adsorption data equally well, yet some of them will not adequately predict the overloaded band profiles.

4.1. Competitive equilibrium isotherms

There is no ''a priori'' criterion leading to the choice of the best isotherm model to which the experimental data should be fitted. Several isotherm models have to be tested successively, beginning by the simplest ones. The best model is decided on the basis of statistical hypothesis tests. The adsorption data obtained in this work were fitted to the four following competitive isotherms:

(1) Langmuir (L):

$$q_i = \frac{q_s K_i c_i}{1 + K_1 c_1 + K_2 c_2} \quad i = 1, 2 \tag{3}$$

where K_i represents the equilibrium constant between the stationary and the mobile phase concentrations and q_s is saturation capacity;

(2) BiLangmuir (BL) with five parameters:

$$q_i = \frac{q_{ns} K_{ns} c_i}{1 + K_{ns}(c_1 + c_2)} + \frac{q_s K_i c_i}{1 + K_1 c_1 + K_2 c_2} \quad i = 1, 2 \tag{4}$$

where the first term on the right-hand side refers to

the non-selective sites (subscript ns) while the second term refers to the selective sites (see below);

(3) Langmuir–Freundlich (LF):

$$q_i = \frac{q_s K_i c_i^{\nu_i}}{1 + K_1 c_1^{\nu_1} + K_2 c_2^{\nu_2}} \quad i = 1, 2 \tag{5}$$

where ν_1 and ν_2 represent the so-called heterogeneity parameter, respectively, for the first and the second component;

(4) Tóth (T):

$$q_i = \frac{q_s K_i c_i}{[1 + (K_1 c_1 + K_2 c_2)^{\nu}]^{1/\nu}} \quad i = 1, 2 \tag{6}$$

where the same heterogeneity parameter, ν, is now used for both components. As follows from Eqs. (3)–(6), the same saturation capacity is assumed for both enantiomers in all the models. In the case of the BL model (Eq. (4)), this condition is extended to both sites. This assumption could appear too restrictive if applied to the competitive isotherms of any pair of compounds. This is much less so in the case of enantiomers, however. Thus, we need to discuss this problem successively from the general viewpoint and from the one of chiral separations. The requirement that competitive isotherms have the same saturation capacity for the components involved in the competitive equilibrium originates from the application of the Gibbs Duhem equation to gas–solid adsorption equilibria in the case of Langmuir competitive isotherms [18]. These isotherms are not thermodynamically consistent if the condition of equal saturation capacities is not fulfilled. However, many sets of experimental adsorption data show quite a different behavior. The column saturation capacities are often not the same for the components of a mixture [2,19]. The problem is solved by applying a more complex isotherm model, for example the ideal adsorbed solution (IAS) theory developed by Myers and Prausnitz [20]. This model was applied by LeVan and Vermeulen in the case in which both components follow a Langmuir or Freundlich isotherm when pure but with different saturation capacities [21]. Using this method, Golshan Shirazi et al. [22] in the case of *cis* and *trans*-androsterone, Quiñones et al. [19] in that of three basic drugs, buspirone, doxepin and diltiazem, obtained excellent predictions of the competitive adsorption behavior from the mere single component isotherms. Because the LeVan–Vermeulen formalism does not introduce any new coefficients, its use merely makes numerical calculations slightly more complex which is not a serious problem today. Nevertheless, if we are to derive the general competitive isotherm model only from data obtained with the 1:1 mixture, this complication is not welcome.

The case of enantiomeric separation appears quite different. First, there are always numerous nonselective sites on a CSP and the saturation capacity of these sites is obviously the same for both enantiomers [23]. Second, the saturation capacity of the chiral-selective sites is often the same or nearly the same for the two enantiomers, while the equilibrium constants are very different [2,23]. Empirical competitive adsorption isotherms written according to Eqs. (3)–(6) seem then adequate for these specific cases [10]. From a numerical point of view, the assumption of Eqs. (3)–(6) permits the estimation of all the competitive isotherm parameters by using only the racemic mixture. They have been used successfully in many different cases [2,23–26].

Table 1 reports the best values obtained for the different parameters of the isotherm models investigated. These values were calculated using an implementation of the non-linear least-squares Marquardt Levenberg algorithm. Also reported in Table 1 is the sum of the squares of the residuals (FSSR) between the experimental data and the theoretical isotherm models considered. The FSSR values give an estimate of the goodness of the fit. They can be used to calculate the Fisher test (*F*-test), which compares the precision of two sets of data by the ratio of their variances [27]. The results of the *F*-test are also reported in Table 1. They are expressed as ''passed'' or ''not passed'' depending on whether the assumption that the null hypothesis *i.e., that the two variances are not significantly different* is accepted (passed) or not (not passed). The BL isotherm was chosen as the reference for this purpose (as it follows from Table 1 that the BL and LF isotherms are characterized by the smallest FSSR values). In other words, a ''not passed'' *F*-test indicates that the corresponding isotherm introduces a significantly larger error in the data fitting than the BL model. The confidence level of the *F*-test was chosen at 95%; the number of degrees of freedom was always

Table 1
Isotherm parameters (concentrations in g/l)

Isotherm model	Parameters	Final sum of squares of residuals, FSSR	Fisher test result[a]
Langmuir	$q_s = 83.1 \pm 1.8$ $K_1 = 0.0777 \pm 0.0023$ $K_2 = 0.0904 \pm 0.0027$	0.274	Not passed
BiLangmuir	Non-selective site $q_{ns} = 98.5 \pm 7.5$ $K_{ns} = 0.0518 \pm 0.0086$ Selective site $q_s = 7.2 \pm 2.4$ $K_1 = 0.176 \pm 0.027$ $K_2 = 0.416 \pm 0.074$	0.069	–
Langmuir–Freundlich	$q_s = 97.7 \pm 4.5$ $K_1 = 0.0633 \pm 0.0034$ $K_2 = 0.0758 \pm 0.0041$ $\nu_1 = 0.9864 \pm 0.0095$ $\nu_2 = 0.9461 \pm 0.0092$	0.066	Passed
Tóth	$q_s = 124 \pm 30$ $K_1 = 0.055 \pm 0.011$ $K_2 = 0.064 \pm 0.013$ $\nu = 0.789 \pm 0.097$	0.238	Not passed

[a] Actual versus BiLangmuir isotherm (see the text for details).

larger than 29 (it changes according to the number of isotherm parameters estimated). Finally, the experimental data regarding competitive adsorption (symbols) and the competitive BL isotherm which best fits these data (continuous line) are reported in Fig. 1. The competitive L model (Eq. 3) should always be considered first [2], when the plot of the experimental adsorption data (plot of the stationary phase versus the mobile phase concentration) is convex upward. The great advantage of this model is the small number of parameters required and the simplicity of its derivation. In fact, only three parameters are needed to describe competitive adsorption: two equilibrium constants and the saturation capacity. In the present case (PP separation on cellulose tribenzoate CSP), however, the competitive L model introduces a larger error in the fit of the experimental data than the BL isotherm, as indicated by the F-test result (Table 1).

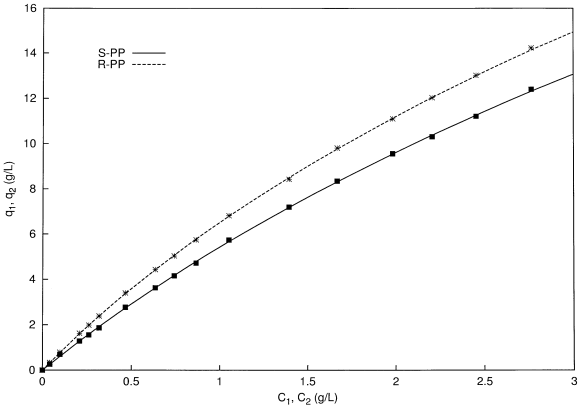

Fig. 1. Experimental competitive adsorption data (symbols) and best BiLangmuir competitive isotherm (solid lines).

The competitive BL model can be considered as an extension of the competitive L model when two kinds of adsorption sites coexist on the surface of the stationary phase [2]. Although far from describing the real complexity of any adsorption surface [28], the BL isotherm appears suitable to account for the mixed retention mechanism often observed in chiral separations [29,30,2,31]. In this case, the two kinds of sites observed are the enantioselective and the

non-selective sites. A diastereomeric reversible equilibrium takes place on the selective sites while the retention of the enantiomers on the non-selective sites is the same. Thus, the equilibrium constants of the two enantiomers on the non-selective sites are equal and the BL model has only five parameters in this case. The relative amount of selective and non-selective sites on the adsorbent surface can be estimated from the data reported in Table 1. From the ratio of the saturation capacities (q_s versus q_{ns} in Table 1), it follows that only about 7% of the surface is covered by selective sites. On them, the PP adsorption is stronger than on the nonselective sites (larger equilibrium constants), the R-PP enantiomer being retained more than twice as much as the S-PP enantiomer. A relatively low proportion of selective sites and a slower adsorption–desorption kinetics on the selective than on the non-selective sites is a result that agrees well with our current understanding of retention on CSPs [1,2,32,33].

In the LF and the T models, the adsorption surface is considered heterogeneous. The degree of this heterogeneity is described by the heterogeneity parameter, ν, with $0 \leq \nu \leq 1$, $\nu = 1$ indicating a completely homogeneous surface (both LF and T models then reduce to the L isotherm). From a physical point of view, the difference between models of heterogeneous and homogeneous surfaces is substantial. With the former models, the surface energy distribution function is continuous (a Gaussian distribution in the LF isotherm, a skewed asymmetrical distribution in the T model [28]). In the latter case, the energy distribution function is represented by an infinitely narrow and high spike (Dirac δ function) for the L case, by two such functions in the BL case. Accordingly, models assuming a heterogeneous surface are more realistic.

The F-test indicates that there are no significant differences between the quality of the fits obtained with the LF and the BL models and that both these models are better than the T model. The LF model (Eq. 5) introduces two heterogeneity parameters: ν_1 for the first enantiomer and ν_2 for the second one. It assumes two Gaussian energy distribution functions, with different first moments (related to the adsorption equilibrium constant) and variances (related to the heterogeneity parameter). The Gaussian distribution relative to S-PP is very narrow ($\nu_1 \simeq 1$), indicating that the surface appears to be almost homogeneous for this compound. In contrast, for R-PP, the adsorption energy spectrum is slightly dispersed ($\nu_2 = 0.95$). Thus, the LF model essentially leads to the same conclusions as the BL model in indicating a small amount of selective interactions with respect to the non-selective ones (both heterogeneity parameter values only slightly differ from the unity). Also, the LF model suggests different chiral recognition mechanisms for the two enantiomers: the diastereomeric interactions for R-PP being stronger and more complex than those for S-PP, as indicated by the more dispersed range of adsorption energies in the R-PP case, certainly involving multi-point interactions and possibly a multi-step kinetic [34,35].

The main inconvenience of the LF isotherm is that it has an infinite Henry constant, hence predicts an infinite retention time at infinite dilution [2]. Fig. 2 shows the results of the band profile calculations for a 5-μl injection (3.9 g/l racemic mixture concentration) when the LF isotherm is used. These are the same experimental conditions used in Fig. 3 where, however, the BL isotherm is assumed (see later). As expected, a very elongated tail appears for R-PP, the compound whose heterogeneity parameter is significantly different from 1. The agreement between the experimental and calculated profiles is much less satisfactory than in the case of the BL model (Fig. 3). The same trend was observed in all the other cases (results not presented here). For these reasons,

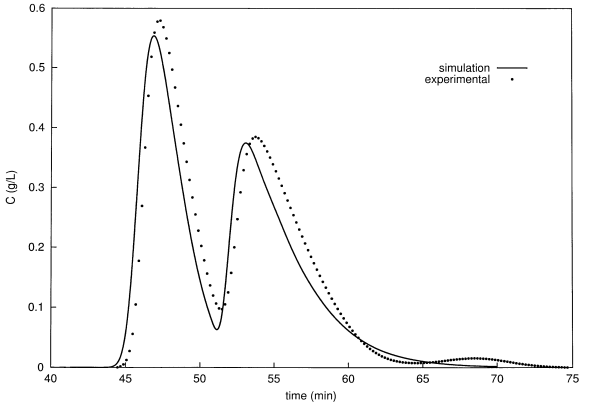

Fig. 2. Comparison between experimental (symbols) and calculated (continuous line) profiles when the Langmuir–Freundlich competitive isotherm is used. Racemic mixture concentration, ≃3.9 g/l; injection volume, 5 μl.

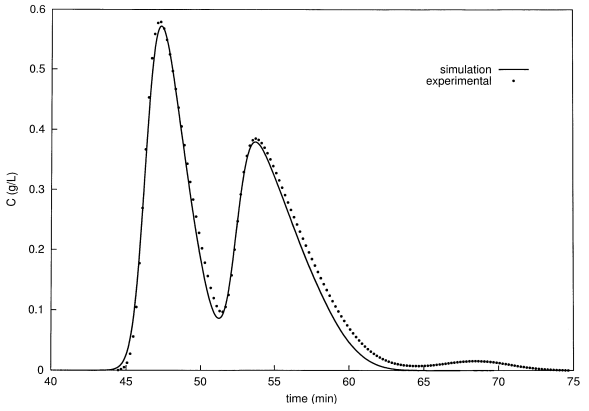

Fig. 3. Comparison between experimental (symbols) and calculated (continuous line) profiles; BL competitive isotherm. Racemic mixture concentration, $\simeq 3.9$ g/l; injection volume, 5 μl; $L = 0.8\%$.

we preferred the BL isotherm model to account for our experimental adsorption data.

4.2. Prediction of band profiles

Figs. 4–6 compare experimental band profiles (solid lines) with those calculated (symbols) using the BL isotherm model and the ED chromatography model (Eq. (1)). The chromatograms were obtained under different experimental conditions and for different values of the loading factors, L_f. L_f was calculated according to the conventional expression [2]:

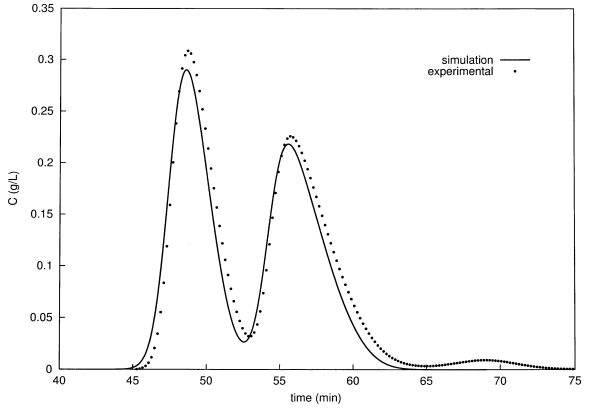

Fig. 4. Comparison between experimental (symbols) and calculated (continuous line) profiles; BL competitive isotherm. Racemic mixture concentration, $\simeq 2$ g/l; injection volume, 5 μl; $L = 0.4\%$.

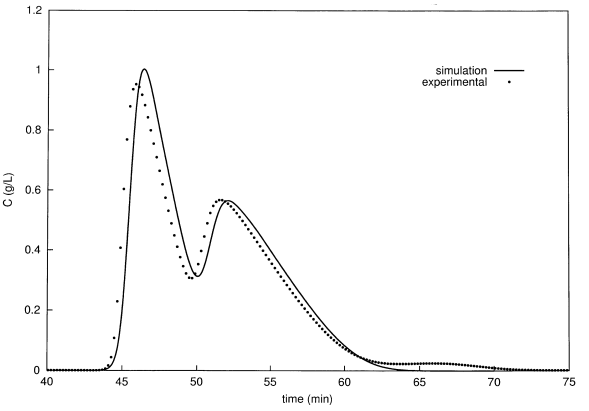

Fig. 5. Comparison between experimental (symbols) and calculated (continuous line) profiles; BL competitive isotherm. Racemic mixture concentration, $\simeq 3.5$ g/l; injection volume, 10 μl; $L = 1.4\%$.

$$L_f = \frac{Q}{(1-\epsilon)SLq_s} \tag{7}$$

where Q is the amount of sample injected into the column and S the column cross-section area. The saturation capacity in Eq. (7) was calculated as the sum of the saturation capacities of the selective and non-selective sites. The agreement between experimental data (points) and calculated profiles (continuous lines) was satisfactory in all cases (L_f (%) = 0.4; 0.8; 1.4; 1.8). Note in all the experimental chromatograms (solid lines) the elution around 65

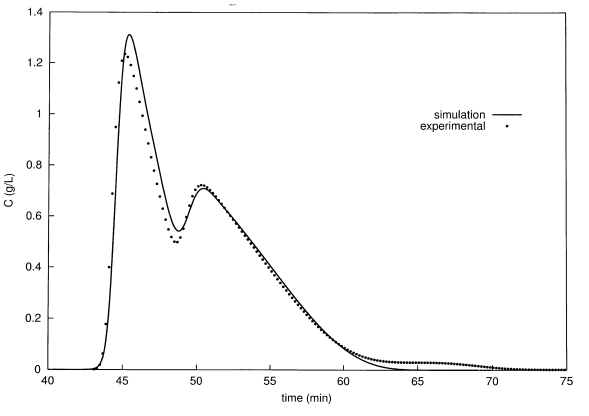

Fig. 6. Comparison between experimental (symbols) and calculated (continuous line) profiles; BL competitive isotherm. Racemic mixture concentration, $\simeq 4.6$ g/l; injection volume, 10 μl; $L = 1.8\%$.

min of a third peak, corresponding to impurity. Although the PP mixture was previously purified, the complete elimination of this impurity (concentration lower than than 1%) was not possible. Its UV absorption was much stronger than that of PP at the wavelengths used. However, because its concentration was actually very low, it did not truly compete with it for adsorption. The agreement between the positions of the peak maxima (calculated versus experimental) was always excellent (the relative error is smaller than 1%). The small differences observed may be explained by minor flow-rate fluctuations related to the injection of the large sample volumes (250 μl) required in FA (see earlier, in Section 3). Another significant difference (up to 5%) is observed between the areas of the calculated and experimental peak (see Figs. 4–6). These differences can be explained by a slight error on the actual amount injected and a larger calibration error (5–7%). Although the detector was calibrated each time overloaded profiles were recorded, the calibration curves are strongly nonlinear, even at low concentrations and this strongly affected the measurements.

4.3. Single component equilibria

The equations describing competitive adsorption isotherms (Eqs. (3)–(6)) are related to single component models [2,36,37]. They should remain valid, with the same isotherm parameters (equilibrium constant, saturation capacity values) when the concentration of one of the component vanishes and a single component model is needed. In fact, although the competitive adsorption data were measured for the racemic mixture, the BL isotherm model was already successfully used to predict the band profiles of large samples of the racemic mixture (Figs. 4–6), a case in which the relative concentration of the two components varies widely during elution. The isotherm showed in Fig. 1 represents only the planar section ($C_1 = C_2$) of a three-dimensional surface, where the stationary phase concentration for one component is expressed as a function of the mobile phase concentrations of both components. So, we already suspect that the same model can be used to account for the adsorption of the pure components, as observed in other cases previously [8]. To demonstrate this property accurately, a systematic study of the adsorption equilibrium at different relative values of C_1 and C_2 should be performed [19]. However, because of all the knowledge previously acquired in this case, it is sufficient to show that the chromatograms recorded for large samples of the pure enantiomers (R-PP and S-PP) can be correctly predicted using the single component isotherms derived from the competitive isotherms determined for the racemic mixture.

Using the BL isotherm that fits best the experimental data, we obtain as model of the single component isotherm:

$$q_i = \frac{q_{ns} K_{ns} c_i}{1 + K_{ns} c_i} + \frac{q_s K_i c_i}{1 + K_i c_i} \quad i = 1, 2 \tag{8}$$

Figs. 7 and 8 compare calculated and experimental band profiles for the S-PP and the R-PP enantiomers, respectively (continuous lines for the calculated profiles, symbols for the experimental data). In general, the agreement between the two sets of profiles is excellent. The only major differences are due to the presence of impurities polluting the single component samples. As obvious in Fig. 8, the R-PP sample is polluted by two impurities: some S-PP enantiomer (eluted as the shoulder on the front of the R-PP profile) and a late eluted impurity at 65 min that was present in the racemic mixture also. Both the retention time and the height of the profile are well predicted. In the case of S-PP (see Fig. 7), the

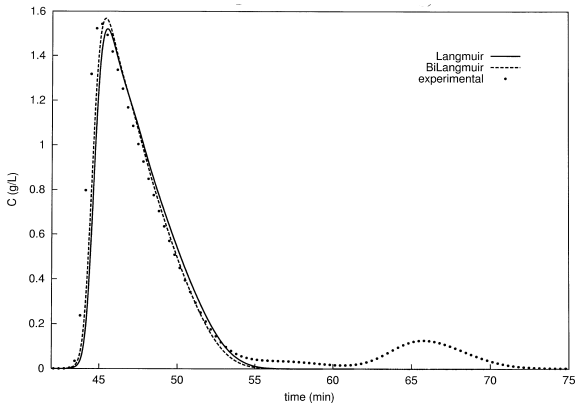

Fig. 7. Comparison between experimental and calculated profiles for S-PP. Symbols, experimental data; dashed line, BiLangmuir model; continuous line, Langmuir model. Pure enantiomer concentration. ≃3.5 g/l; injection volume, 10 μl.

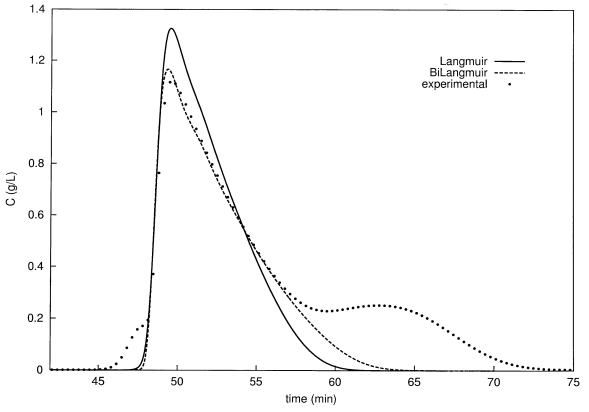

Fig. 8. Comparison between experimental and calculated profiles for R-PP. Symbols, experimental data; dashed line, BiLangmuir model; continuous line, Langmuir model. Pure enantiomer concentration, ≃3.4 g/l; injection volume, 10 μl.

position of the calculated shock matches closely the experimental data and a small tag-along effect [2] can be observed.

Two other calculated profiles (dashed lines) are shown in Figs. 7 and 8. They represent the calculation results obtained when a single component L isotherm model is used to account for the adsorption behavior of the pure component with

$$q_i = \frac{q_s K_i c_i}{1 + K_i c_i} \quad i = 1, 2 \tag{9}$$

Although the L isotherm is not the best model to account for the adsorption behaviour of PP on cellulose tribenzoate, it is interesting to observe that, in the case of S-PP (Fig. 7), the profile calculated with the L model agrees well with the experimental one. A quite different result is obtained for the R-PP enantiomer (Fig. 8). This gives a further clue that the adsorption mechanism for S-PP and R-PP is quite different.

4.4. Scaling up

The results reported above are the first demonstration that narrow bore columns can be used to acquire sufficiently accurate isotherm data and to predict overloaded band profiles in good agreement with those calculated from these isotherms. In the light of these satisfactory results the following question arises: Is it possible to use the isotherm parameters obtained with a microbore column to simulate the separation on a analytical (or preparative) scale column? Recently, some of us [10] studied the adsorption equilibrium of the PP racemic mixture on a 20 × 1.0-cm column packed with the same stationary phase as used in this study (Chiracel OB, 20 μm particle diameter). For the sake of simplicity, it is convenient to compare the results obtained with the two columns by merely using a competitive L model which requires only three parameters. The fact that this is not the best model to account for the experimental data in either case [10] is not very important: because the fitting of the experimental data to the competitive L isotherm was more than satisfactory. For the analytical column, the following parameters were obtained [10]: saturation capacity $q_s = 46.9 \pm 1.0$, equilibrium constants for the first and the second components, $K_1 = 0.0865 \pm 0.0026$ and $K_2 = 0.1102 \pm 0.0033$. A comparison of these data with those in Table 1 shows an important difference. The saturation capacity in the microbore column is almost twice as large as that in the analytical column and there is approximately a 10% difference between the equilibrium constants.

The other parameters measured on the analytical and the microbore column also yielded quite different results. The permeability of the microbore column is much larger than that of the analytical column. The total porosity was 0.795 for the microbore column and only 0.715 for the analytical one. These differences are not surprising, however. They can be explained by differences in packing density, easily explained by the fact that for the microbore column there are only about 50 particles per column diameter versus more than 200 for the analytical column. This may explain differences in permeability and external porosity [38]. In our opinion, the major reason leading to these unexpected differences between the properties of the two columns is related to the fact that the analytical column was used for 2 years in an SMB unit and had been operated under very different experimental conditions [17]. In particular, the use of ethyl acetate as a mobile phase modifier [17] is not advised with cellulose tribenzoate CSP, because of its relatively strong adsorption on the surface [1]. This could have caused enough changes in some of the adsorption sites [34,35] and,

at least partially, explain the different values measured for the saturation capacities. Further experimental investigations are in progress to clarify this point.

5. Conclusions

Accurate competitive isotherm data could be measured on a microbore HPLC column by competitive frontal analysis. Once again, the competitive BL model was shown to account well for the adsorption equilibrium data obtained for PP on cellulose tribenzoate CSP. This suggests that the surface of this CSP can be depicted as covered by two kinds of adsorption sites: enantioselective and nonselective sites. The former are in smaller amount and the adsorption kinetic, different for R-PP and S-PP, is slower on them than on nonselective sites. These results agree with other experimental data [2] which show that a mixed retention mechanism often works well for enantiomeric separations. In the case of PP, it seems also that the enantioselective adsorption mechanism is different for the two chiral compounds. In fact, only the adsorption mechanism of the more retained enantiomer truly requires a mixed kinetic. The behavior of the less retained enantiomer (S-PP) could well be described by a simpler model. The use of a more sophisticated adsorption model, the LF isotherm that fits equally well to the experimental data, lead to a very similar conclusion.

We also showed that the equilibrium isotherm model derived from competitive data obtained with the racemic mixture applies well to a wide range of relative concentrations of the two enantiomers and can even be used to model the single component equilibria. This was satisfactorily demonstrated by comparing the calculation results obtained using the best competitive isotherm model to account for single component behavior and the experimental profiles recorded for large samples of single component solutions. The use of a microbore column allows a consistent reduction of the amount of sample needed as well as of the mobile phase consumption. Additionally, the amount of packing material required to pack the column is much smaller which is particularly important in chiral separations, given the extremely high costs of the CSPs [1]. With respect to analytical columns [10], a cost reduction by a factor 10 could easily be reached.

Acknowledgements

This work was supported in part by grant CHE-00-70548 of the National Science Foundation and by the cooperative agreement between the University of Tennessee and the Oak Ridge National Laboratory. The support of the whole staff of Agilent Technologies concerned with the development and maintenance of the 1100 Cap column is gratefully acknowledged, particularly that of Gerard P. Rozing.

References

[1] S. Ahuja, in: Chiral Separations by Chromatography, Oxford University Press, Washington, DC, 2000.
[2] G. Guiochon, S.G. Shirazi, A. Katti, in: Fundamentals of Preparative and Nonlinear Chromatography, Academic Press, Boston, MA, 1994.
[3] D.U. Staerk, A. Shitangkoon, E. Winchester, G. Vigh, A. Felinger, G. Guiochon, J. Chromatogr. A 734 (1996) 155.
[4] D.U. Staerk, A. Shitangkoon, E. Winchester, G. Vigh, A. Felinger, G. Guiochon, J. Chromatogr. A 734 (1996) 289.
[5] R.P.W. Scott, Adv. Chromatogr. 22 (1983) 247.
[6] J.P.C. Vissers, H.A. Claessens, C.A. Cramers, J. Chromatogr. A 779 (1997) 1.
[7] P. Jandera, S. Bunčeková, K. Mihlbachler, G. Guiochon, V. Bačkovská, J. Planeta, J. Chromatogr. A 925 (2001) 19.
[8] D.E. Cherrak, S. Khattabi, G. Guiochon, J. Chromatogr. A 877 (2000) 109.
[9] K. Kaczmarski, D. Antos, H.G. Sajonz, P. Sajonz, G. Guiochon, J. Chromatogr. A 925 (2001) 1.
[10] A. Cavazzini, K. Kaczmarski, P. Szabelski, D. Zhou, G. Guiochon, Anal. Chem. 73 (2001) 5704.
[11] K. Kaczmarski, G. Storti, M. Mazzotti, M. Morbidelli, Comput. Chem. Eng. 21 (1997) 641.
[12] J.A. Berninger, R.D. Whitley, X. Zhang, N.H.L. Wang, Comput. Chem. Eng. 15 (1991) 749.
[13] P.N. Brown, A.C. Hindmarsh, G.D. Byrne, Variable coefficient ordinary differential equation solver procedure, available on http://ntelib.org.
[14] M. Martin, G. Blu, G. Guiochon, J. Chromatogr. Sci. 11 (1973) 641.
[15] M. Martin, G. Blu, C. Eon, G. Guiochon, J. Chromatogr. 112 (1975) 399.
[16] M. Martin, G. Guiochon, J. Chromatogr. 151 (1978) 267.
[17] S. Khattabi, D.E. Cherrack, J. Fisher, P. Jandera, G. Guiochon, J. Chromatogr. A 877 (2000) 95.

[18] C. Kemball, E.K. Rideal, E.A. Guggenheim, Trans. Faraday Soc. 44 (1948) 948.
[19] I. Quiñones, A. Cavazzini, G. Guiochon, J. Chromatogr. A 877 (2000) 1.
[20] A.L. Myers, J.M. Prausnitz, AIChE J. 11 (1965) 121.
[21] M.D. LeVan, T. Vermeulen, J. Phys. Chem. 85 (1981) 3247.
[22] S. Golshan-Shirazi, J.-X. Huang, G. Guiochon, Anal. Chem. 63 (1991) 1147.
[23] T. Fornstedt, P. Sajonz, G. Guiochon, Chirality 10 (1998) 375.
[24] T. Fornstedt, G. Gotmar, M. Andersson, G. Guiochon, J. Am. Chem. Soc. 121 (1999) 1164.
[25] S. Khattabi, D.E. Cherrak, J. Fischer, G. Guiochon, J. Chromatogr. A 877 (2000) 95.
[26] D. Zhou, D.E. Cherrak, A. Cavazzini, K. Kaczmarski, G. Guiochon, Chem. Eng. Sci., in press
[27] A. Felinger, in: Data Analysis and Signal Processing in Chromatography, Elsevier, Amsterdam, 1998.
[28] W. Rudziński, D.H. Everett, in: Adsorption of Gases On Heterogeneous Surfaces, Academic Press, New York, 1992.
[29] G. Götmar, T. Fornstedt, G. Guiochon, Chirality 12 (2000) 558.
[30] S. Jacobson, S. Golshan-Shirazi, G. Guiochon, J. Am. Chem. Soc. 112 (1990) 6492.
[31] P. Jandera, V. Bačkovská, A. Felinger, J. Chromatogr. A 919 (2001) 67.
[32] T.E. Beesley, R.P.W. Scott, in: Chiral Chromatography, Wiley, Chichester, 1998.
[33] G. Subramanian (Ed.), A Practical Approach To Chiral Separations By Liquid Chromatography, VCH, Weinheim, 1994.
[34] I.W. Wainer, M.C. Alembik, J. Chromatogr. 358 (1986) 85.
[35] I.W. Wainer, R.M. Stiffin, T. Shibata, J. Chromatogr. 411 (1987) 139.
[36] G.M. Schwab, in: Ergebnisse der Exacten Naturwissenschaften, Vol. 7, Springer, Berlin, 1928.
[37] E.C. Markham, A.F. Benton, J. Am. Chem. Soc. 53 (1931) 497.
[38] T. Farkas, G. Zhong, G. Guiochon, J. Chromatogr. A 849 (1999) 35.